Optimization of Operational Cost for a Grid-Supporting PV System With Battery Storage

Iromi Ranaweera[a,*], Ole-Morten Midtgård[a]

[a] *Department of Electric Power Engineering, Norwegian University of Science and Technology (NTNU), 7491 Trondheim, Norway*

Abstract

Coupling an energy storage to a photovoltaic (PV) system not only increases the self-consumption but also solves the over-voltage issues if the cycling of the storage is properly controlled. Whatever the application the storage is used for, the primary concern of the system owner is to maximize the profits. Therefore, this paper addresses an energy management system for a PV system coupled with battery energy storage, which maximizes the daily economic benefits while curtailing the power injection to the grid in such a way that helps to mitigate over-voltage problems caused by reverse power flow. A time dependent grid feed-in limit is proposed achieve this objective. The daily operational cost that includes the energy cost and the battery degradation cost is considered as the objective function. The non-linear constrained optimization problem is solved using dynamic programming. The analyses are made to investigate the economic benefits of charging the battery from the grid. It is found that there is a possibility for these systems for participating in load-levelling if batteries are charged from the PV system. In order for that to be feasible, the peak-hour sell-back price for the energy from storage should be higher than the off-peak utility electricity price.

Keywords: Dynamic programming, energy management, load-levelling, photovoltaic systems, voltage quality

1. Introduction

Building integrated PV systems have continued to make rapid progress around the world over the past few years. Increasing the PV penetration level in the low voltage (LV) grid creates several technical issues mainly related to the power quality [1–4]. The most critical problem is the voltage rise because of the reverse power flow [5]. A significant percentage of the energy generated from the PV system is injected into the grid because of weak correlation between residential load and the power production from the PV system. This results in reverse power flow. In the early stages, power curtailment was used to deal with this problem [6, 7]. Even though this is a feasible solution, this increases the payback time of the PV system because

*Corresponding author. Tel.: +47 73 59 4269
Email addresses: iromi.ranaweera@ntnu.no (Iromi Ranaweera), ole-morten.midtgard@ntnu.no (Ole-Morten Midtgård)

part of the energy generation from the system is wasted. Later, new standards came in to effect such as VDE-AR-N 4105 [8], allowing inverters to operate in voltage regulation mode by absorbing reactive power from the grid when the power injection from the PV system goes above a certain threshold [9]. However, as the number of PV generators connected to the LV grid increases, the total losses in the network will also increase as a result of higher consumption of reactive power by the PV inverters [10–12].

The power penetration into the grid from renewable energy systems especially wind and solar is increasing rapidly. The power output of these systems is highly intermittent and fluctuating in nature. As the total capacity of such sources becomes significant, the complexity of controlling the system increases. Therefore, utilities will need to adopt energy storage solutions to help integrate these renewable sources into the grid [13, 14]. The future grid essentially requires energy storage to balance the generation and consumption as well as to maintain the grid stability. The main applications of grid level storage are capacity firming, spinning reserve, load-levelling, improving power quality, and frequency regulation [15, 16].

Recently, a growing trend to increase the self-consumption in residential level PV systems has been observed. This is mainly due to customers' desire for independence from the grid electricity, continuous increases in electricity prices, a decrease in feed-in-tariffs, and various kinds of incentives provided in some countries. According to IHS technology, a tenfold increase in the global market demand for residential PV systems coupled with battery energy storage (BES) is expected over the next three years, where the current capacity is 90 MW.Currently, lithium-ion batteries dominate this market. The major barrier preventing the market from taking off is the high price of the lithium-ion batteries. However, a reduction in the average price is expected in the coming years, making storage more attractive. In addition to increasing self-consumption, these small systems can have several other applications: improving power quality, peak shaving, and load-levelling. Whatever the application they are being used for, the system owner's primary objective is to increase the economic benefits besides energy independence. Therefore, if these systems are going to be used for utility applications, a profitable business case should be available from the utility side and a proper energy management system that maximizes the economic benefits should be available from the system owner's side.

Several studies have been presented on the literature on the topic of optimal energy management for grid-connected PV systems coupled with energy storage. All of them involve solving optimization problems subject to certain constraints, assuming the day-ahead forecasts of load profile, PV power production profile, and the energy prices are available. The objective function varies depending on the application of the storage, and the choice of the optimization algorithm depends on the complexity of the objective function and the constraints. In [17], the optimum energy dispatch schedule is found where the storage is utilized for peak shaving. The main purpose is to minimize the demand charge. The net energy exchanged with the grid over the planning horizon has been considered as the objective function, and the dispatch schedule that minimizes the objective function has been found using linear programming. Ref. [18] also describes the

optimum dispatch schedule with the same purpose, but there the objective function is the energy cost. The peak shaving is achieved by setting a constraint on the power drawn from the grid. As they have considered different tariffs for energy from the PV and the grid, the objective function becomes non-linear, hence dynamic programming is used to solve the optimization problem. Ref. [19] presents optimal control strategies for battery storage considering different objectives such as maximizing battery life, maximizing self-consumption, and minimizing energy cost. They have also used dynamic programming. Ref. [20] addresses the problem of over-voltages due to reverse power flow. They minimize the net power injection to the grid over the planning horizon using quadratic programming aiming to minimize the impact on the grid from PV systems. In addition, they also maximize the economic benefits by introducing selectable weights in the objective function which are calculated based on greedy-search heuristic algorithm.

In this work, our objective is to maximize the economic benefits for the system owner while optimally contributing to over-voltage mitigation in the grid. Further, we investigate whether residential PV systems coupled with BES can participate in grid load-levelling and identify the requirements for utilizing them for such applications. A scenario where a distribution grid has a high PV penetration, but with limited storage, is considered. As the amount of storage is limited, the objective is to use it optimally, storing as much power as possible, while giving high priority to the period where the over-voltage issues are most likely to occur. Two different configurations of a residential PV system coupled with BES have been considered for the sake of comparison of the performances.

The paper is organized as follows. Section 2 describes the system configuration and Section 3 presents the methodology used. Section 4 details the mathematical formulation of the problem and Section 5 describes the application of dynamic programming for solving the optimization problem. Finally, results of a simulation study are provided in section 6, and we conclude that the proposed algorithm can successfully optimize the operational cost while limiting the power injection into the grid helping it to mitigate possible over-voltage issues caused by high PV penetration.

2. System Configuration

Two different configurations of residential PV systems coupled with BES can be found: DC- and AC-coupled systems [21]. In a DC-coupled system, the battery bank is connected to the intermediate DC link directly or through a bi-directional converter. The grid converter could be bi-directional if the batteries are supposed to be charged not only from the PV array but also from the grid. In a AC-coupled system, the battery bank and the PV array are connected to the AC bus via a bi-directional battery converter and an inverter respectively. Fig. 1 illustrates the two different configurations. In this study, both configurations are considered in order to compare the performances. The grid converter in the DC-coupled configuration is considered bi-directional.

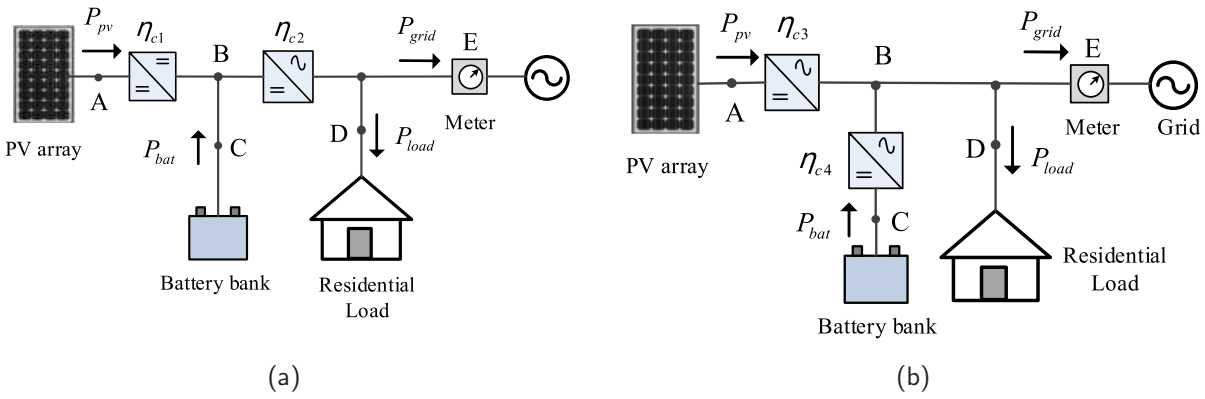

Figure 1: Configurations of PV systems coupled with batteries (a) DC-coupled, (b) AC-coupled. Arrows indicate the direction of positive power flow.

3. Methodology

Our objective is to maximize the economic benefits for the system owner while helping the grid to maintain the voltage profile within acceptable level. The cause of the voltage rise problem is the reverse power flow due to high PV power penetration. However, it should be noted that the PV production profile over the day approximately takes the shape of a quadratic function having maximum around solar noon, on a clear sky day. Hence, PV systems affect the grid voltage quality principally around solar noon. Having energy storage units in the network, the active power injection into the grid can be controlled. As stated in the introduction, in this study we consider a case with a significant amount of PV penetration but a limited amount of storage. As not all the PV generators are coupled with BES, the existing storage units should be optimally controlled so that the negative impact on the grid voltage quality is minimized. In this work, we do not consider coordinated control of energy storage units. Instead, we optimize the operation of the individual PV systems with BES independently.

The system has a hierarchical control, in which the optimization or the energy management layer lies on top. Every day before midnight, the energy management system (EMS) optimizes the scheduling of the battery bank for the next 24 hours using the forecasted load profile, PV generation profile and the day-ahead electricity pricing information. The EMS calculates the average power transfer to the battery and the energy transfer over the selected time intervals and sends this information to the power management system. Then the power management system calculates instantaneous references (power references, current references and/or voltage references) for the component level controllers.

4. Mathematical Formulation of the Problem

The notations used to represent the power flow averaged over a specific time interval of Δt measured at points A, C, D, and E are represented in Fig. 1 along with the sign convention. The arrows in the figure

indicate the direction of positive power flow. According to this sign convention, battery discharging and power injection into the grid are considered as positive. $\eta_{cj}, j = \{1, 2, 3, 4\}$ represents the efficiencies of the converters adopted in two different configurations. A typical efficiency characteristic of a power electronic converter is shown in Fig. 2. Usually this is available in the product data sheet. It can be represented by a rational function

$$\eta = \frac{a_1 P_n^2 + a_2 P_n + a_3}{P_n + b_1}, \tag{1}$$

where $P_n = \dfrac{P_{out}}{P_{rated}}$, P_{out} is the converter output power, P_{rated} is the converter rated output power and a_1, a_2, a_3, b_1 are constants.

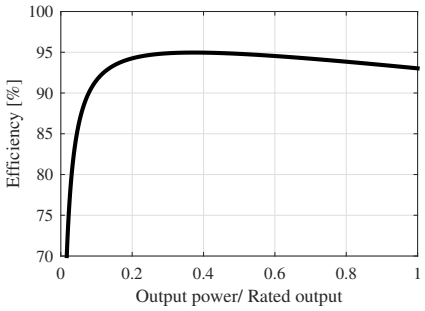

Figure 2: Typical efficiency characteristic of a power electronic converter.

For the system shown in Fig. 1(a), the power balance equation at the k^{th} time step: $\{k \in \mathbb{Z}^+\}$ can be written as follows:

$$\eta_{c1}\ P_{pv}(k) + P_{bat}(k) = \begin{cases} \dfrac{P_{load}(k) + P_{grid}(k)}{\eta_{c2}} \\ ; \eta_{c1}\ P_{pv}(k) + P_{bat}(k) \geq 0 \\ \eta_{c2}\big(P_{load}(k) + P_{grid}(k)\big) \\ ; \eta_{c1}\ P_{pv}(k) + P_{bat}(k) < 0 \end{cases} \tag{2}$$

For the system shown in Fig. 1(b), the power balance equation is:

$$\eta_{c3}\ P_{pv}(k) = \begin{cases} P_{load}(k) + P_{grid}(k) - \eta_{c4}\ P_{bat}(k) \\ \qquad ;\ P_{bat}(k) \geq 0 \\ P_{load}(k) + P_{grid}(k) - \dfrac{P_{bat}(k)}{\eta_{c4}} \\ \qquad ;\ P_{bat}(k) < 0 \end{cases} \tag{3}$$

The operation of the system components is limited by a set of physical constraints including rated power, rated capacity, maximum current, and maximum and minimum voltage. In a DC-coupled configuration, the

battery discharging and charging rate is determined by the ratings of the battery itself. In addition, the power flow through the grid converter should be below or equal to the grid converter rating. Hence, for the DC-coupled configuration the following constraints hold.

Battery constraints:

$$-I_{chrg,rated} \leq I_{bat}(k) \leq I_{dischrg,rated} \tag{4}$$

Grid converter constraints:

$$\begin{aligned} \eta_{c1}\ P_{pv}(k) + P_{bat}(k) &\leq P_{conG,rated} \\ P_{grid}(k) + P_{load}(k) &\geq -P_{conG,rated} \end{aligned} \tag{5}$$

$I_{chrg,rated}$ is the rated charging current and $I_{dischrg,rated}$ is the rated discharging current of the battery. $P_{conG,rated}$ is the rated capacity of the grid converter.

In the AC-coupled configuration, the battery charging/discharging rate is determined by the battery converter rating, given that the rated charging/discharging capacity of the battery is below the battery converter rating.

$$-\eta_{c4}\ P_{conB,rated} \leq P_{bat}(k) \leq P_{conB,rated}\ , \tag{6}$$

where $P_{conB,rated}$ is the rated capacity of the battery converter.

The state of charge (SOC) of the battery should be maintained within certain limits to prolong the battery lifetime. This constraint does not depend on the configuration and can be stated as follows.

$$SOC_{min} \leq SOC(k) \leq SOC_{max} \tag{7}$$

The net energy transfer from the battery during a planning horizon is set to zero, in order to maintain the continuity of the battery operation. This constraint can be represented as follows.

$$\sum_{k=1}^{N} P_{bat}(k)\ \Delta t = 0 \tag{8}$$

or

$$SOC(0) = SOC(N)$$

N is the total number of discrete intervals per optimization time horizon. $N = \frac{T}{\Delta t}$, where T is the optimization time horizon.

4.1. Battery State of Charge

Fig. 3 illustrates the steady state equivalent circuit of the battery where E_b is the open circuit voltage (OCV) and R_{bat} is the internal resistance. In this study, we consider a lithium-ion battery. The open circuit voltage vs the SOC characteristic of a lithium-ion battery (12 V,100 AH - SB100 from Smart Battery company) is shown in Fig. 4. Unlike other battery types, the voltage profile of a lithium-ion battery is very

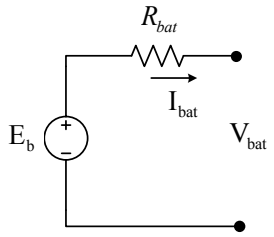

Figure 3: Equivalent battery model.

flat in the SOC range 20-90 %, and the voltage is relatively high close to the fully charged state. High voltages cause the cells to deteriorate, therefore shortens the battery lifetime. Hence, it is not desirable to fully charge lithium-ion batteries. As the OCV over the acceptable operating range does not vary significantly, it can assumed to be constant. Then the battery voltage is:

$$V_{bat} = E_b - I_{bat} R_{bat}, \tag{9}$$

where a negative I_{bat} means a battery charging.

From coulomb counting, the SOC of the battery at the k^{th} time step $k = \{1, 2, 3, ..., N\}$ can be found as: $I_{bat}(k) < 0$ (charging):

$$SOC(k) = SOC(k-1) - \frac{\eta_{chrg}\, I_{bat}(k)\, \Delta t}{C_{bat}}\,, \tag{10}$$

$I_{bat}(k) > 0$ (discharging):

$$SOC(k) = SOC(k-1) - \frac{I_{bat}(k)\, \Delta t}{\eta_{dischrg}\, C_{bat}}\,, \tag{11}$$

where C_{bat} is the nominal capacity or the usable capacity of the battery in Ah, whereas η_{chrg} and $\eta_{dischrg}$ are the charging and discharging efficiencies (coulomb efficiency) of the battery, respectively. The battery efficiency depends on the battery current. It is lower at higher currents and vice versa. However, for simplification we assume that the battery efficiency is constant at different operating conditions. Further, we assume that the charging and discharging efficiencies of the battery are the same and equal to the square-root of the battery round-trip efficiency ($\eta_{bat,rt}$).

$$\eta_{chrg} = \eta_{dischrg} = \sqrt{\eta_{bat,rt}}$$

The usable battery capacity drops as the battery ages mainly because of cycling and calendrical ageing. It is also influenced by various other factors such as inefficient charging, excessive charging voltages, deep discharging, and temperature. The state of health (SOH) indicates the current usable battery capacity with respect to the nominal capacity of the battery when it was new. The impact of battery capacity variation because of ageing should be taken into account when calculating the SOC. However, over the planning horizon it can be assumed constant as the planning horizon is typically a short period (e.g. a day). But at

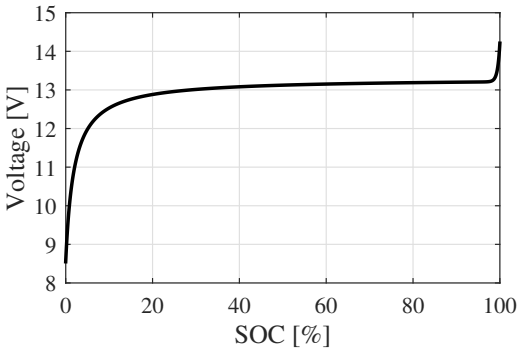

Figure 4: Open circuit voltage of a lithium-ion battery vs SOC.

the end of the day, the SOH should be taken into account for the next planning horizon. Either an analytical model or a measurement based model can be used to estimate the SOH of the battery [22–24].

4.2. Grid Constraints

As mentioned before, in this study we consider a distribution grid with high PV penetration, but where the number of storage units is much less than the number of PV systems. The clear-sky solar resource over the day is deterministic with the peak around solar noon, therefore, the over-voltage problem principally occurs at this time. The optimal way to use the storage to eliminate the power quality problem is to store as much power as possible during peak generation hours and less at other times. Generally, the grid feed-in is limited to a constant threshold level, or the inverters are operated in voltage regulation mode by absorbing reactive power from the grid when the power injection to the grid exceeds the threshold. Having storage units reduces the need for voltage control based on reactive power absorption, because the system can control the active power injection to the grid, the origin of the problem.

Instead of setting a constant value for the upper limit of the variable P_{grid}, we propose a time-dependent upper limit as follows.

$$P_{grid,ub}(k) = \begin{cases} a(k - K_{sn})^2 + P_{grid,ub,min} \\ \qquad ; K_m \leq k \leq K_e \\ P_{grid,ub,max} \\ \qquad ; \text{otherwise} \end{cases} \tag{12}$$

where $P_{grid,ub}(k) \geq 0$ and K_{sn} $\{K_{sn} \in \mathbb{Z}^+\}$ is found from the solar noon time T_{sn} as:

$$K_{sn} = \frac{T_{sn}}{\Delta t}$$

K_m and K_e $\{K_m, K_e \in \mathbb{Z}^+\}$ are given by

$$K_m = \frac{T_{sn} - \Delta t_{pk}/2}{\Delta t} \; ; \; K_e = \frac{T_{sn} + \Delta t_{pk}/2}{\Delta t}$$

Δt_{pk} is the peak generation period and $P_{grid,ub,max}$ is the maximum value of the upper limit of the grid power injection as shown in Fig. 5. These two parameters are set constant for a given system. $P_{grid,ub,min}$ is the minimum value of the upper limit of the grid power injection and it depends on the load and the generation profile. The method for choosing the optimal value for this parameter is described in Section 5.1. In this way, the time around the peak generation hour (with respect to the generation profile on a clear-sky day) is given highest priority. Therefore, we utilize the existing storage units in an optimal way so that the power injection into the grid during the hours of high PV generation is minimized.

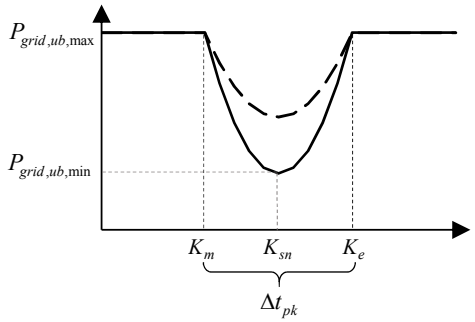

Figure 5: An adjustable, time-dependent grid feed-in limit.

4.3. Electricity Bill

The most common pricing mechanisms for residential PV systems are feed-in-tariffs (FITs), net billing, and net metering [25, 26]. Under a FIT mechanism, a guaranteed price is paid for all the electricity produced by the system and electricity is bought at a standard price to supply the residential load. In net metering, customers are billed for their net energy at the end of the billing period. The net billing system measures energy in and out separately including time stamp, therefore can account the TOU dynamic electricity price when calculating the cost of energy. In this study, we consider the net billing mechanism with a flat sell-back price for the energy feed-in to the grid from the PV system. A TOU energy price is applied for the energy from the utility and the energy from the storage. The following notations are used to denote the different electricity prices.

$\gamma_b(k)$ - TOU utility electricity price.

$\gamma_{s,pv}$ - Flat sell-back price for PV system generated electricity.

$\gamma_{s,bat}(k)$ - TOU sell-back price for the energy from the storage.

The energy feed into the grid at the k^{th} time interval can comprise energy from the PV array as well as energy from the battery. The cost of energy flowing through the meter (E) in Fig. 1 can be calculated as follows, where $C(k)$ denotes the billed cost for the k^{th} time interval.

1. Power is fed into the grid and battery is discharging: $P_{grid}(k) \geq 0$ and $P_{bat}(k) \geq 0$

DC-coupled configuration:

$$C(k) = \begin{cases} (\eta_{c1}\eta_{c2}P_{pv}(k) - P_{load}(k))\Delta t\ \gamma_{s,pv} \\ +\eta_{c2}\ P_{bat}(k)\Delta t\ \gamma_{s,bat}(k) \\ \qquad\qquad ;\eta_{c1}\eta_{c2}P_{pv}(k) > P_{load}(k) \\ P_{grid}(k)\ \Delta t\ \gamma_{s,bat}(k) \\ \qquad\qquad ;\eta_{c1}\eta_{c2}P_{pv}(k) \leq P_{load}(k) \end{cases}$$

AC-coupled configuration:

$$C(k) = \begin{cases} (\eta_{c3}P_{pv}(k) - P_{load}(k))\Delta t\ \gamma_{s,pv} \\ +\eta_{c4}\ P_{bat}(k)\Delta t\ \gamma_{s,bat}(k) \\ \qquad\qquad ;\eta_{c3}P_{pv}(k) > P_{load}(k) \\ P_{grid}(k)\ \Delta t\ \gamma_{s,bat}(k) \\ \qquad\qquad ;\eta_{c3}P_{pv}(k) \leq P_{load}(k) \end{cases}$$

2. Power is fed into the grid and battery is charging: $P_{grid}(k) \geq 0$ and $P_{bat}(k) < 0$

$$C(k) = P_{grid}(k)\ \Delta t\ \gamma_{s,pv}$$

3. Power is drawn from the grid: $P_{grid}(k) < 0$

$$C(k) = P_{grid}(k)\ \Delta t\ \gamma_b(k)$$

4.4. Objective Function

The basic objective function is the electricity bill over the planning horizon. However, the battery capacity degrades over the time due to cycling and calendrical ageing. Inclusion of battery degradation cost (BDC) due to cycling prevents unnecessary cycling of the battery that can be triggered by slight changes in the electricity cost. Further, inclusion of BDC due to calendrical ageing avoids holding the operation of the battery until higher economic benefit is achieved.

The BDC per kWh energy discharge from the battery due to cycling is calculated from the equation

$$\gamma_{bat,cyl} = \frac{\text{BC}}{\text{E}_{bat,ltpt}},$$

where BC is the battery installation and maintenance cost over its lifetime. $\text{E}_{bat,ltpt}$ is the lifetime throughput of the battery and given by

$$\text{E}_{bat,ltpt} = \text{E}_{avg} \times \text{DOD} \times \text{Number of cycles to failure},$$

where E_{avg} is the average battery capacity over the lifetime and it can be calculated by averaging the battery capacity when it is new and the end of its life time. The threshold of the end of life capacity is generally 80 % of the nominal capacity; however, it can vary depending on the application, user preference and the manufacture policy. DOD is the depth of discharge of the battery. $\gamma_{bat,cycling}$ is derived based on the linear relationship between the battery capacity and the number of equivalent full discharges obtained from the experimental results [27]. As this linear relationship is obtained for discharged cycles, we assume that the capacity degrades only during discharging. As a result, the BDC due to cycling can be expressed as follows.

$$\mathrm{BDC}_{cyl}(k) = \begin{cases} \gamma_{bat,cyl}\ P_{bat}(k)\Delta t & ; P_{bat}(k) > 0 \\ 0 & ; P_{bat}(k) \leq 0 \end{cases} \tag{13}$$

Calendrical ageing of the battery occurs when it is not operating. The rate of ageing is affected by SOC and the temperature. The measurements of SOH changes for $LiFePO_4$ battery at different temperature and SOC levels has been presented in [28, 29]. The following relationship is obtained for SOH changes per hour based on this results alone with the assumption that the temperature remains constant.

$$\Delta\mathrm{SOH} = a\ [\mathrm{SOC}]^2 + b\ [\mathrm{SOC}] + c\ , \tag{14}$$

where a, b, c are constants. From the expression it can be seen that the calendrical ageing of the battry is higher at higher SOC. The BDC per 1 kWh capacity loss of the battery can be found from the equation

$$\gamma_{bat,calAg} = \frac{\mathrm{BC}}{\mathrm{E}_{bat} - \mathrm{E}_{\mathrm{EOL}}}\ ,$$

where E_{bat} is the nominal capacity [kWh] of the battery when it is new and $\mathrm{E}_{\mathrm{EOL}}$ is the end of life capacity [kWh] of the battery. Then the BDC due to calendrical ageing can be found from the following equation.

$$\mathrm{BDC}_{calAg}(k) = \gamma_{bat,calAg} \times \Delta\mathrm{SOH}(k) \times \mathrm{E}_{bat} \times \Delta t \tag{15}$$

The objective function takes the following form when including the BDC due to cycling and calendrical ageing.

$$\text{Objective function} = \sum_{k=1}^{N} C(k) - \underbrace{\mathrm{BDC}_{cyl}(k)}_{\text{when } P_{bat}(k) \neq 0} - \underbrace{\mathrm{BDC}_{calAg}(k)}_{\text{when } P_{bat}(k) = 0} \tag{16}$$

The objective is to maximize the economic benefit for the user. Note that, according to the sign convention used, power injection to the grid is positive. Hence, in order to maximize the economic benefit for the user, we need to maximize the objective function.

5. Optimization Using Dynamic Programming

The non-linear constrained optimization problem is solved using dynamic programming [30]. In dynamic programming, the optimization problem is structured into multiple stages, where each stage is comprised of collective states. Recursive optimization is adopted with the backward induction process, where the final stage is analysed first and the problem is solved moving back one stage at a time until all stages are included. In our problem, the stages represent different time periods in the problem's planning horizon, and discretized SOC with a step size of SOC_{step} corresponds to the states of the system. The number of stages is N and the number of states per stage is

$$\frac{SOC_{max} - SOC_{min}}{SOC_{step}}$$

Fig. 6 illustrates all possible trajectories for change in SOC from one stage to the other from the initial stage up to three stages. As shown in the figure, the allowable range of variation for the SOC is between SOC_{min} and SOC_{max} to fulfil the constraint given in Eq. (7). Further, the SOC at the beginning and the end of the time period must be the same to satisfy the the constraint given in Eq. (8). In the figure, ΔSOC_{ij} represents the change in SOC along the trajectory from the i^{th} state in the k^{th} stage to the j^{th} state in the $(k+1)^{th}$ stage.

$$\Delta SOC_{ij} = SOC_i(k) - SOC_j(k+1)$$

After establishing all possible trajectories, corresponding ΔSOC_{ij} values are calculated. Then, the average currents flowing in or out over all trajectories are calculated from the following equations.
$\Delta SOC < 0$ (charging):

$$I_{bat} = \frac{C_{bat}}{\eta_{chrg}\,\Delta t}\,\Delta SOC_{ij}$$

$\Delta SOC \geq 0$ (discharging):

$$I_{bat} = \frac{C_{bat}\,\eta_{dischrg}}{\Delta t}\,\Delta SOC_{ij}$$

While doing this, all the trajectories that violate the constraint given in Eq. (4) are rejected. Then the average power flowing to/from the battery is calculated from

$$P_{bat} = V_{bat} I_{bat}\ ,$$

where the battery voltage is found using Eq. (9).

Next, the average power transfer from/to the grid is calculated from Eq. (2) and Eq. (3) for DC- and AC-coupled configurations, receptively. At this point, all the trajectories that violate the grid feed-in limitation described in Eq. (12) and the constraints given in Eqs. (5) and (6) are rejected. After that, the associated cost over all feasible trajectories are calculated from Eq. (16). Then, the optimum trajectory from stage 0 to stage N, which results in maximum cost, is found using backward induction.

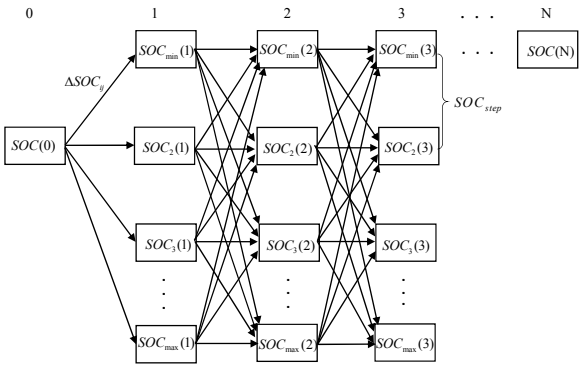

Figure 6: Dynamic programming: System stages, states and all possible trajectories between the stages.

5.1. Calculating the Optimal Value for the Minimum Limit of Grid Power Injection

In order to optimally utilize the energy storage units to minimize the negative impact on the grid, the power injection to the grid should be minimized. To achieve this objective, we propose a time-dependent grid feed-in limit as shown in Fig. 5. As our requirement is to minimize the grid feed-in as much as possible, the optimum value for $P_{grid,ub,min}$ should be zero. However, when the net energy (difference between the energy production from the PV array and the load) over the planning horizon is relatively high, the optimization problem does not have a solution that satisfies all the constraints for a very low value of $P_{grid,ub,min}$ because of the limited capacity of the battery. Therefore, we start the optimization described in Section 5 with $P_{grid,ub,min} = 0$, and if no solution satisfying all constraints is found, $P_{grid,ub,min}$ is increases step-wise until convergence is reached. The corresponding value found for $P_{grid,ub,min}$ is the optimal value. That is, we get the minimum energy injection to the grid at this optimal value. For a given battery capacity, the optimal value of $P_{grid,ub,min}$ depends on the PV profile and the load profile; hence it can take different values for different days.

6. Results and Discussion

Simulations were carried out for a residential PV system with BES to investigate the effectiveness of the proposed optimum energy management algorithm. Table 1 lists the parameters of the studied system and Fig. 7 illustrates the efficiency characteristics of the converters adopted in two different configurations. The daily domestic electrical load profiles over a year were obtained from IEA/ECBCS Annex 42 [31]. We assumed that these load profiles correspond to electric load profiles of a residential application in southern Norway. The measured power production from a PV module with a peak capacity of 300 W installed on a PV test station at the University of Agder in the town of Grimstad is used as the basis for the PV production profiles [32]. Daily production profiles from a 4.2 kWp PV array were generated by scaling up the data

obtained from the 300 Wp module. The simulation model of the optimum EMS was developed in Matlab. The parameters used in the simulation model are listed in Table 2.

Table 1: Parameters of the Studied System.

Parameter	Value
PV array size	4.2 kWp
Nominal battery capacity	300 Ah/15 kWh
OCV of the battery bank	52.8 V
battery internal resistance	5 mΩ
$P_{conG,rated}$	4.2 kW
$P_{conB,rated}$	5 kW
Battery round trip efficiency	95 %
SOC_{max}	90 %
SOC_{min}	20 %
$\gamma_{bat,cycling}$	0.4 $/kWh
$\gamma_{bat,calenderAg}$	3200 $/kWh
ΔSOH coefficients (a,b,c)	3.333×10^{-5}, 2.083×10^{-5}, 8.333×10^{-6}

Table 2: Parameters Used in the Simulation.

Parameter	Value
Initial SOC	20 %
Optimization time horizon (T)	24 hours
Simulation time step (Δt)	1 hour
SOC_{step}	0.4 %
$P_{grid,ub,max}$	2 kW
peak hour period (Δt_{pk})	7 hours

Simulations were carried out for three different cases:(1) a case without separate sell-back price for the energy from the storage for a day with less production from the PV system, (2) a case without separate sell-back price for the energy from the storage for a day with high production from the PV system, (3) a case with separate sell-back price for the energy from the storage.

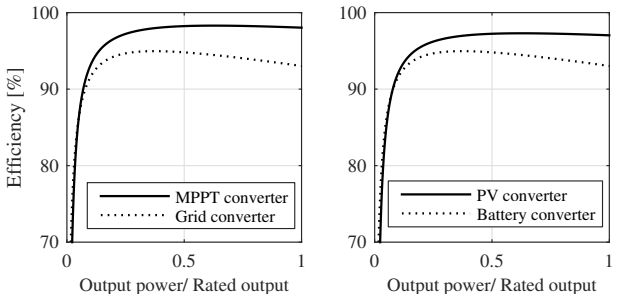

Figure 7: Efficiency characteristics of the converters: Converters in the DC-coupled configuration are shown to the left, and the converters in the AC-coupled configuration are shown to the right.

Case 1: Without separate sell-back price for the energy from the storage for a day with less production from the PV system

In this case, the grid does not differentiate the energy directly fed from the PV array and the battery. The utility electricity prices fluctuate over the day in which high prices corresponding to the time-period of most heavily loaded grid. In this study we considered two distinct prices as shown in Fig. 8, which reflect the time the grid is lightly and heavily loaded. A day with relatively low production from the PV array was simulated to investigate the economic viability of charging the battery from the grid during the low price period, and discharge during the high price period to supply the local demand. The economically optimum cycling profile of the battery obtained for this case is shown in Fig. 8. As can be seen, for the given price variation, the economical optimum operation is to let the battery remain idle, i.e. not to charge from the grid in the morning when the price is low. This is because the price variation is not large enough to recover the battery degradation cost and the cost of lost energy in the converters and battery. However, it is important to investigate under which conditions it becomes economical to charge the battery under TOU energy tariff. This is because if distributed storage units are going to be used for load levelling applications, then the pricing scheme should provide economic benefits for the system owners.

The amount of energy that must be drawn from the grid for the battery at a later stage to feed Q [kWh] amount of energy to the local load or back to the grid is

$$\frac{Q}{\eta_{ck}^2\ \eta_{bat,rt}}\ \text{kWh},$$

where $k = 2$ or 4 depending on the configuration shown in Fig. 1.

The associated cost for buying the energy from the grid and battery degradation cost due to cycling when assuming battery capacity degrades only during discharging is

$$Q\left(\frac{\gamma_{b,\textit{off-peak}}}{\eta_{ck}^2\ \eta_{bat,rt}} + \frac{\gamma_{bat,cyl}}{\eta_{ck}\ \sqrt{\eta_{bat,rt}}}\right),$$

where $\gamma_{b,\textit{off-peak}}$ is the utility electricity price during off-peak hours.

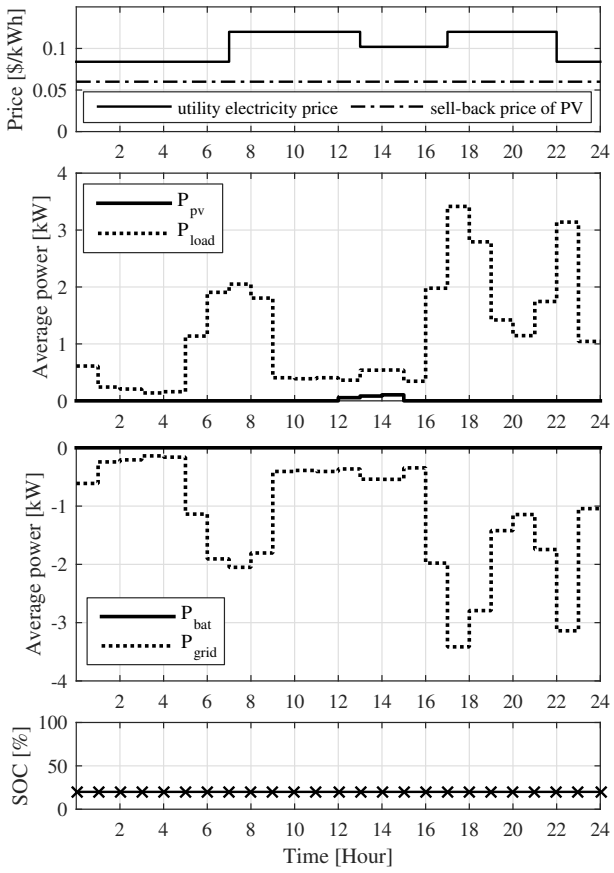

Figure 8: Electricity prices, power profiles and the battery SOC variation on a day with relatively small energy production from the PV system. There is no separate sell-back price for the energy from the battery. All the energy injected to the grid is paid the sell-back price of PV.

The money saved or earned from feeding Q amount of energy to the local load or the grid is

$$Q\,\gamma_{b,peak} + \gamma_{bat,calenderAg}\,\Delta T\ ,$$

where $\gamma_{b,peak}$ is the utility electricity price during peak hours and ΔT is the total operating time of the battery (charging and discharging) for handling the energy. The battery operation is economically beneficial for the system owner if

$$\gamma_{b,peak} + \gamma_{bat,calAg}\frac{\Delta T}{Q} \geq \frac{\gamma_{b,off\text{-}peak}}{\eta_{ck}^2\ \eta_{bat,rt}} + \frac{\gamma_{bat,cyl}}{\eta_{ck}\ \sqrt{\eta_{bat,rt}}}.$$

Rearranging the above expression we get

$$\gamma_{b,peak} - \frac{\gamma_{b,off\text{-}peak}}{\eta_{ck}^2\ \eta_{bat,rt}} \geq \frac{\gamma_{bat,cyl}}{\eta_{ck}\ \sqrt{\eta_{bat,rt}}} - \gamma_{bat,calAg}\frac{\Delta T}{Q}. \tag{17}$$

Instead of holding the battery for a long time, circulating certain amount of energy during that time can make the right hand side of the above expression much smaller than the left hand side, hence making cycling of the battery more economical than remain idle.

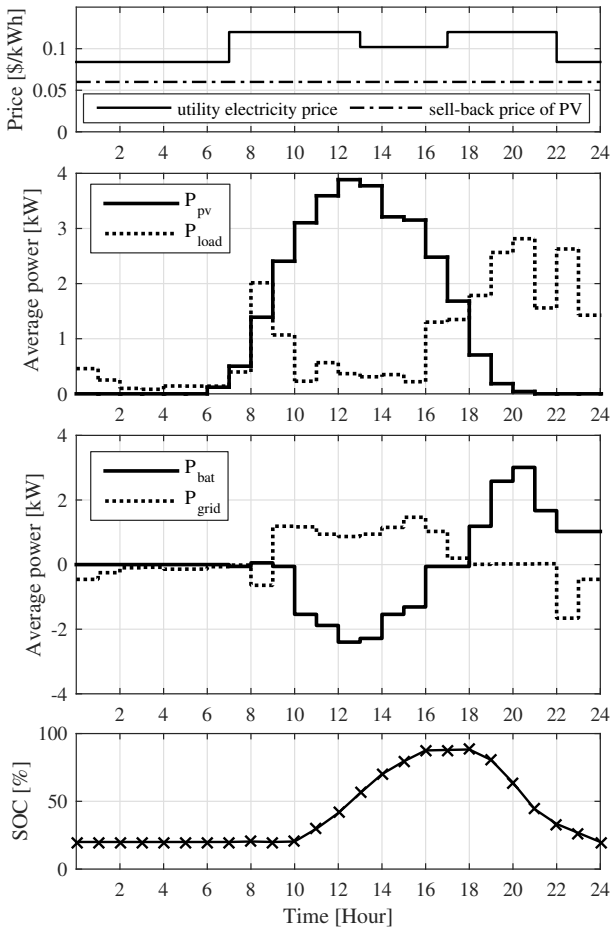

Figure 9: Electricity prices, power profiles and the battery SOC variation on a typical clear summer day. There is no separate sell-back price for the energy from the battery. All the energy injected to the grid is paid the sell-back price of PV.

Case 2: Without separate sell-back price for the energy from the storage for a day with high production from the PV system

A case with a slightly different utility electricity price variation compared to case 1 was considered for a day with high energy production from the PV system. Fig. 9 illustrates the considered price variation, power profiles and the corresponding optimum cycling profile of the battery. As the energy production from the PV array is higher compared to the load, the system injects about 0.5 kW of average power during the peak generation hour. The power injection into the grid follows the grid feed-in limit profile shown in Fig. 5, which tries to minimize the power injection as much as possible while giving high priority to hours around the peak sunshine hour. As described in Section 5.1, the optimization algorithm starts with zero for the minimum value of the grid feed-in limit and increases it step-wise until convergence is reached. Therefore, the battery is forced to charge to the maximum SOC limit whenever the total net energy production is higher than the battery capacity even though the battery degradation cost is higher compared to the sell-back rate.

The system utilizes all the energy stored in the battery to supply the local load. It is not economical to inject energy stored in the battery to the grid because of the low sell-back price, particularly when the sell-back price is even lower than the off-peak electricity price. Therefore, with this pricing mechanism the utility cannot utilize the energy stored in the residential storage during peak hours for load-levelling. Even though storage does not inject energy into the grid during peak hours, it indirectly participate for grid load-levelling by reducing the local peak-hour demand, because the local demand is supplied by the energy from the storage.

Case 3: With separate sell-back price for the energy from the storage

In this case, different sell-back price for the energy injected from the storage to the grid is introduced, which allow utility to draw energy from the residential storage due to higher economic benefits for the system owner against local consumption. The considered utility electricity price, sell-back price for the energy from the PV system and the storage is shown in Fig. 10. Here, we considered a varying utility price that reflects the peak and off-peak hours of the utility as before. As the grid needs energy from the storage during peak hours, a high sell-back price which follows the same variation as the utility electricity price was considered. As the grid does not need energy from the storage during off-peak hours, off-peak sell-back price was set to zero. Fig. 10 illustrates the economical optimum charging-discharging profile obtained for the battery. In this case, more economic benefits can be gained by injecting all the excess energy into the grid during peak hours. The battery reaches the minimum SOC limit at the end of the peak period. Therefore, the local off-peak demand is fully supplied by the grid. This operation is economically beneficial for the system owner as long as the peak hour sell-back price for the energy from the storage is higher than the off-peak utility electricity price. Hence, if the utility wants to draw energy from the residential storage units in the distribution grid during peak-hours, then the utility should buy energy from the storage at a price which is higher than the off-peak utility electricity price. Nevertheless, in addition to injecting excess energy into the grid, the storage indirectly participates in grid load-levelling by reducing local electricity demand during peak hours, because it is fully supplied by the storage.

6.1. Operation of the Battery for Consecutive Days

In the above study, we have selected 24 hours as the planning period and 1 hour as the time step. However, both parameters can be changed depending on the availability of load and PV production forecasts. Fig. 11 illustrates the results obtained for planning period of 3 days. On the second day, the power generation from the PV system is relatively small when compared to the load. Therefore, instead of discharging the battery to minimum SOC level by the end of the first day, keeping the energy to supply the following day peak-time load results higher economic benefits. However, PV and load forecasts of several days are required in order to shift the energy among consecutive days. If we allow end of the day SOC to be flexible without knowing

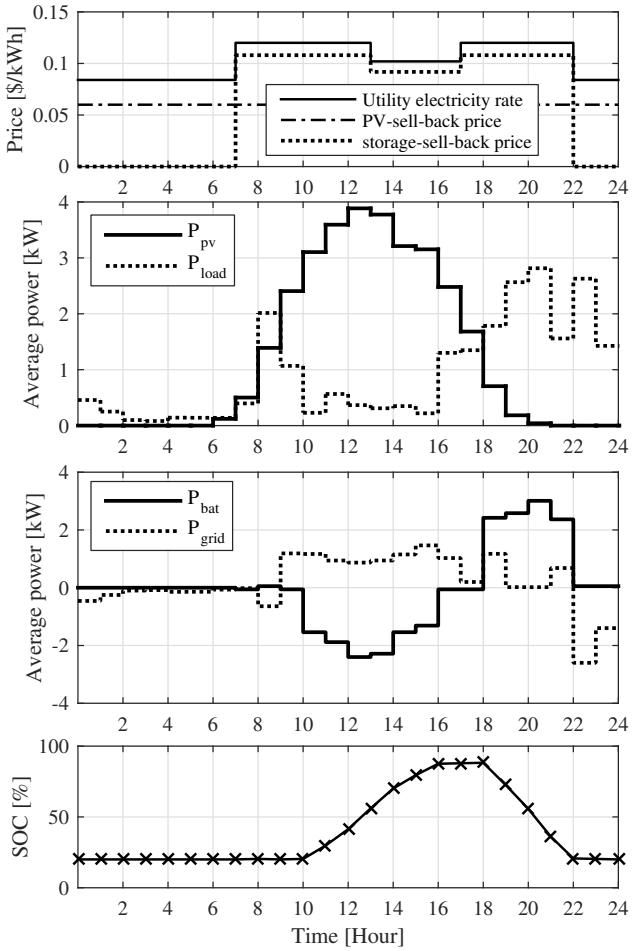

Figure 10: Electricity prices, power profiles and the battery SOC variation on a typical clear summer day with separate sell-back price for the energy from the battery.

the forecasts of the following day, then the EMS will attempt to reduce discharging of the energy from the battery due to higher battery cycling degradation cost compared to the electricity price and the calendrical ageing battery degradation cost.

6.2. Comparison of Economics Between the Two System Configurations

Optimum operational costs of DC- and AC-coupled systems were calculated in order to compare the performance of the two different system configurations. Fig. 12 illustrates the daily operational cost of two different configurations for 60 distinctive days. From the results it can be seen that the differences in the daily costs of the two different systems are negligible. Therefore, in terms of daily operational cost, the performance of the both systems are the same. Hence, efficiency of the configuration is not a critical factor to be considered when deciding on a configuration should be chosen. However, the AC configuration has several advantages over the DC configuration. It is more flexible in the planning and development stage,

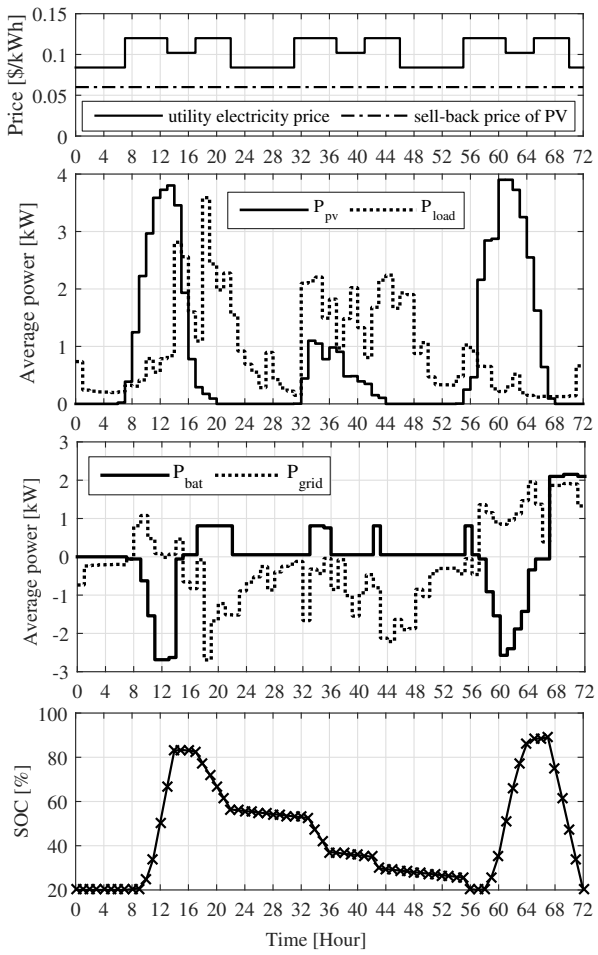

Figure 11: Electricity prices, power profiles and the battery SOC variation for three consecutive days of operation.

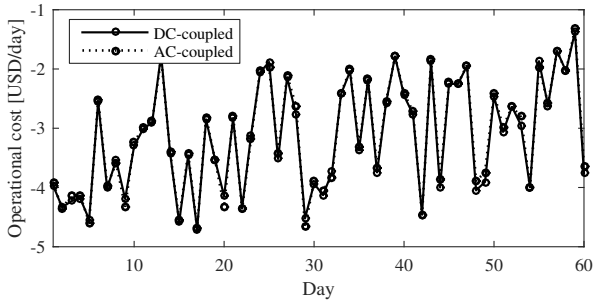

Figure 12: Daily operational cost comparison of AC- and DC-coupled systems.

easily expandable without replacing any converters, and the battery bank and the battery converter can be sized independently of the PV inverter.

7. Conclusion

An optimum energy management system for a battery coupled to a PV system based on dynamic programming, is proposed. The EMS maximizes the economic benefits while curtailing the power injection into the grid in such a way that helps the grid to maintain the voltage profile within the limits during the period of high PV penetration. An adjustable time-dependent grid feed-in limit, which is treated as a constraint in the optimization algorithm, is proposed to minimize the power injection to the grid particularly around peak generation hours. The objective of this is to minimize the reverse power flow that leads to over-voltage issues by utilizing the storage units connected to the grid. The adjustable grid feed-in limit ensures charging the battery to the maximum SOC limit whenever the excess energy is higher than the battery capacity, even though the battery degradation cost is higher compared to the sell-back price.

It is found that the utility has the possibility to buy energy from the residential storage to supply the peak demand as long as they pay a price which is higher than the off-peak electricity price for the energy they buy from the storage. This shows the potential of utilizing residential storage for grid load-levelling. Moreover, the daily energy cost comparison for two common system configurations (DC- and AC-coupled) did not show a significant difference. Therefore, the difference in the overall efficiency of the system does not contribute much to the daily energy cost, hence it should not be a critical factor to be considered when designing the system.

Acknowledgment

Iromi Ranaweera acknowledges the financial support provided by the Norwegian University of Science and Technology for her PhD studies and University of Agder for providing the experimental data set specifically Georgi Hristov Yordanov for his assistance.

References

[1] M. ElNozahy, M. Salama, Technical impacts of grid-connected photovoltaic systems on electrical networks-A review, Journal of Renewable ans Sustainable Energy 5 (3).

[2] V. V. Thong, J. Driesen, Handbook of Power Quality, Wiely, Ch. Supplementary Material, pp. 113–121.

[3] S. Cobben, B. Gaiddon, H. Laukamp, Impact of photovoltaic generation on power quality in urban areas with high PV population, Tech. rep., Intelligent Energy-Europe (2008).

[4] S. Eftekharnejad, V. Vittal, Heydt, B. Keel, J. Loehr, Impact of increased penetration of photovoltaic generation on power systems, IEEE Transactions on Power Systems 28 (2) (2013) 893–901. doi:10.1109/TPWRS.2012.2216294.

[5] E. Caamano, J. Thornycroft, H. Moor, State of the art on dispersed PV power generation: Publication review on the impacts of PV distributed generation and electricity networks, Tech. rep., Intelligent Energy-Europe (2007).

[6] P. Denholm, R. M. Margolis, Evaluating the limits of solar photovoltaics (pv) in traditional electric power systems, Energy Policy 35 (5) (2007) 2852–2861. doi:10.1016/j.enpol.2006.10.014.

[7] T. Stetz, F. Marten, M. Braun, Improved low voltage grid-integration of photovoltaic systems in germany, IEEE Transactions on Sustainable Energy 4 (2) (2013) 534–542. doi:10.1109/TSTE.2012.2198925.

[8] Power generation systems connected to the low voltage distribution network, VDE-AR-N 4015:2011-08, Tech. rep., VDE Association for Electrical, Electronic & Information Technologies (2011).

[9] B. Craciun, T. Kerekes, D. Sera, R. Teodorescu, Overview of recent grid codes for PV power integration, in: International Conference on Optimization of Electrical and Electronic Equipment (OPTIM), 2012.

[10] A. Samadi, R. Eriksson, L. Soder, B. G. Rawn, J. C. Boemer, Coordinated active power-dependent voltage regulation in distribution grids with pv systems, IEEE Transactions on Power Delivery 29 (3) (2014) 1454–1464. doi:10.1109/TPWRD.2014.2298614.

[11] R. Tonkoski, L. A. C. Lopes, T. H. M. El-Fouly, Coordinated active power curtailment of grid connected pv inverters for overvoltage prevention, IEEE Transactions on Sustainable Energy 2 (2) (2011) 139–147. doi:10.1109/TSTE.2010.2098483.

[12] A. Cagnano, E. De Tuglie, Centralized voltage control for distribution networks with embedded pv systems, Renewable Energy 76 (2015) 173–185. doi:10.1016/j.renene.2014.11.015.

[13] P. Munshi, J. Pichel, E. Kwe, Energy storage: Game-changing component of the future grid, Tech. rep., Piper Jaffray Investment Research (2009).

[14] A. Mammoli, H. Barsun, R. Burnett, J. Hawkins, J. Simmins, Using high-speed demand response of building HVAC systems to smooth cloud-driven intermittency of distributed solar photovoltaic generation, in: Transmission and Distribution Conference and Exposition (T D), 2012 IEEE PES, 2012, pp. 1–10.

[15] B. P. Roberts, C. Sandberg, The role of energy storage in development of smart grids, Proceedings of the IEEE 99 (6) (2011) 1139–1144. doi:10.1109/JPROC.2011.2116752.

[16] Y. Ru, J. Kleissl, S. Martinez, Storage size determination for grid-connected photovoltaic systems, IEEE Transactions on Sustainable Energy 4 (1) (2013) 68–81. doi:10.1109/TSTE.2012.2199339.

[17] A. Nottrott, J. Kleissl, B. Washom, Energy dispatch schedule optimization and cost benefit analysis forgrid-connected, photovoltaic-battery storage systems, Renewable Energy 55 (2013) 230–240. doi:10.1016/j.renene.2012.12.036.

[18] Y. Riffonneau, S. Bacha, F. Barruel, S. Ploix, Optimal power flow management for grid connected pv systems with batteries, IEEE Transactions on Sustainable Energy 2 (3) (2011) 309–320. doi:10.1109/TSTE.2011.2114901.

[19] J. Li, M. A. Danzer, Optimal charge control strategies for stationary photovoltaic battery systems, Journal of Power Sources 258 (2014) 365–373. doi:10.1016/j.jpowsour.2014.02.066.

[20] E. L. Ratnam, S. R. Weller, C. M. Kellett, An optimization-based approach to scheduling residential battery storage with solar pv: Assessing customer benefit, Renewable Energy 75 (2015) 123–134. doi:10.1016/j.renene.2014.09.008.

[21] M. H. Nehrir, C. Wang, K. Strunz, H. Aki, R. Ramakumar, J. Bing, Z. Miao, Z. Salameh, A review of hybrid renewable/alternative energy systems for electric power generation: Configurations, control, and applications, IEEE Transactions on Sustainable Energy 2 (4) (2011) 392–403. doi:10.1109/TSTE.2011.2157540.

[22] M.-H. Hung, C.-H. Lin, L.-C. Lee, C.-M. Wang, State-of-charge and state-of-health estimation for lithium-ion batteries based on dynamic impedance technique, Journal of Power Sources 268 (2014) 861–873. doi:10.1016/j.jpowsour.2014.06.083.

[23] D. Andre, C. Appel, T. Soczka-Guth, D. U. Sauer, Advanced mathematical methods of soc and soh estimation for lithium-ion batteries, Journal of Power Sources 224 (2013) 20–27. doi:10.1016/j.jpowsour.2012.10.001.

[24] B. Sun, J. Jiang, F. Zheng, W. Zhao, B. Y. Liaw, H. Ruan, Z. Han, W. Zhang, Practical state of health estimation of power batteries based on delphi method and grey relational grade analysis, Journal of Power Sources 282 (2015) 146–157. doi:10.1016/j.jpowsour.2015.01.106.

[25] A. Poullikkas, A comparative assessment of net metering and feed in tariff schemes for residential pv systems, Sustainable Energy Technologies and Assessments 3 (2013) 1–8. doi:10.1016/j.seta.2013.04.001.

[26] Y. Yamamoto, Pricing electricity from residential photovoltaic systems: A comparison of feed-in tariffs, net metering, and

net purchase and sale, Solar Energy 86 (9) (2012) 2678–2685. doi:10.1016/j.solener.2012.06.001.

[27] A. D. E. Lemaire, F. Mattera, P. Malbranche, Assessment of storage ageing in different types of PV systems: Technical and economical aspects, in: 23rd European Photovoltaic Solar Energy Conference and Exhibition (EU PVSEC), 2008.

[28] A. Farman, Erstellen eines messtechnisch gesttzten modells zur berechnung der kalendarischen alterung von LiFePO4-batterien, Master's thesis, Hochschule Mnchen.

[29] Y. Yang, H. Li, A. Aichhorn, J. Zheng, M. Greenleaf, Sizing strategy of distributed battery storage system with high penetration of photovoltaic for voltage regulation and peak load shaving, Smart Grid, IEEE Transactions on 5 (2) (2014) 982–991. doi:10.1109/TSG.2013.2282504.

[30] R. Bellman, Dynamic Programming, Dover Publications, 2003.

[31] IEA/ECBCS Annex 54- integration of micro-generation and related energy technologies in buildings (2010).
URL http://www.iea-annex54.org/annex42/data.html

[32] A. Imenes, G. Yordanov, O. Midtgard, T. Saetre, Development of a test station for accurate in situ I-V curve measurements of photovoltaic modules in Southern Norway, in: Photovoltaic Specialists Conference (PVSC), 2011 37th IEEE, 2011, pp. 003153–003158.